

A set of 201 rays were launched parallel to the initial target surface; they then traversed the simulated plasma represented by the LASNEX output. The ray deflections were calculated from the LASNEX density profile with Eqs. 1 and 2. Only gradients perpendicular to the target surface were considered; the plasma was assumed to be azimuthally uniform with an initial diameter of 3 mm.

The code results for deflection are compared with the measurements in Fig. 4A. The ray-tracing calculation was carried out with use of the simulated density profile obtained 0.9 ns after the start of the laser pulse that created the target plasma; this corresponds to the peak of the x-ray laser probe beam. The measured deflections show good agreement with theory. The simulation results do predict a very slightly larger deflection at large distances from the target surface.

To compare the LASNEX prediction of the density profile to the experiment, we integrated the index-of-refraction gradient profile. The slope normalization in the deflectogram was carried out as far from the target surface as possible, but at about $x = 500 \mu\text{m}$, we needed to make some assumption about the boundary density n_0 . We could have assumed the density here to be zero, but LASNEX modeling indicated that the density at $x = 500 \mu\text{m}$ is $\sim 10^{20} \text{cm}^{-3}$. Therefore, we plotted two curves, one corresponding to $n_0 = 0$ and another for $n_0 = 10^{20} \text{cm}^{-3}$ (Fig. 4B). There is substantial disagreement between the code prediction and the $n_0 = 0$ curve, but the $n_0 = 10^{20}$ curve agrees with the simulation to within about 40% throughout the corona. At low densities ($n_e < 10^4 \text{cm}^{-3}$) the uncertainty regarding the initial density at the edge of the deflectogram does not presently allow a final comparison with the code predictions; later experiments with increased field-of-view and sensitivity will be required to resolve this issue. At higher densities, the 40% disagreement exceeds the measurement uncertainties. The LASNEX calculations appear to overestimate the electron density in the steady-state part of the corona, confirming comparisons with earlier experiments (8).

REFERENCES AND NOTES

1. J. D. Lindl *et al.*, *Phys. Today* **45**, 32 (September 1992); J. H. Nuckolls *et al.*, *Nature* **239**, 139 (1972).
2. R. P. Drake *et al.*, *Phys. Fluids* **31**, 3130 (1988); C. L. Shepard *et al.*, *ibid.* **29**, 584 (1986); W. C. Mead *et al.*, *ibid.* **26**, 2316 (1983).
3. L. B. Da Silva *et al.*, *Phys. Rev. Lett.* **69**, 438 (1992).
4. J. F. Seely *et al.*, *J. Quant. Spectrosc. Radiat. Transfer* **27**, 297 (1982); C. De Michelis and M. Mattioli, *Nucl. Fusion* **21**, 677 (1981).
5. R. P. Drake *et al.*, *Phys. Fluids B* **1**, 1089 (1989); H. Figueroa, C. Joshi, H. Azechi, N. A. Ebrahim, K. G. Estabrook, *Phys. Fluids* **27**, 1887 (1984).

6. G. E. Busch, C. L. Shepard, L. D. Siebert, J. A. Tarvin, *Rev. Sci. Instrum.* **56**, 879 (1985).
7. O. Kafri and I. Glatt, *The Physics of Moiré Metrology* (Wiley, New York, 1990).
8. E. F. Gabl *et al.*, *Phys. Fluids B* **2**, 2437 (1990); D. Ress, L. J. Suter, E. F. Gabl, B. H. Failor, *ibid.*, p. 2448.
9. R. F. Schmalz and K. Eidmann, *Phys. Fluids* **29**, 3483 (1986); R. F. Schmalz, *ibid.* **28**, 2923 (1985).
10. T. Afshar-Rad *et al.*, *Phys. Rev. Lett.* **68**, 942 (1992); J. S. Schlacter, *Tech. Rep. LA-9333-T* (Los Alamos National Laboratory, Los Alamos, NM, 1982).
11. L. A. Vasil'ev, *Schlieren Methods* (Israel Program for Scientific Translations, New York, 1971).
12. R. S. Craxton *et al.*, *Phys. Fluids B* **5**, 4419 (1993); C. Darrow *et al.*, *J. Appl. Phys.* **67**, 3630 (1990).
13. R. C. Elton, *X-Ray Lasers* (Academic Press, Boston, MA, 1990).
14. E. Keren and O. Kafri, *J. Opt. Soc. Am. A* **2**, 111 (1985).
15. L. B. DaSilva *et al.*, *Opt. Lett.* **18**, 1174 (1993).
16. G. B. Zimmerman and W. L. Krueer, *Comments Plasma Phys. Controlled Fusion* **2**, 85 (1975). LASNEX is primarily a hydrodynamic simulation code. The dynamics of a hot fluid are modeled by a finite-difference solution of Euler's equations. The code also models the deposition of laser energy in the plasma by inverse bremsstrahlung, the transport of x-rays through the material by diffusion, and electron thermal conduction by diffusion.
17. M. K. Prasad *et al.*, *Phys. Fluids B* **4**, 1569 (1992).
18. We gratefully acknowledge the assistance of D. Ciarlo in fabricating the one-dimensional rulings and the Nova two-beam laser-facility crew for performing these experiments. This work was performed under the auspices of the U.S. Department of Energy by Lawrence Livermore National Laboratory under contract W-7405-ENG-48.

23 February 1994; accepted 24 May 1994

Contribution of Early Cells to the Fate Map of the Zebrafish Gastrula

Kathryn Ann Helde,* Ellen T. Wilson,* Chris J. Cretekos, David Jonah Grunwald†

Previously, a tissue-specific fate map was compiled for the gastrula stage of the zebrafish embryo, indicating that development subsequent to this stage follows a reproducible pattern. Here it is shown that each early zebrafish blastomere normally contributes to a subset of the gastrula and thus gives rise to a limited array of tissues. However, the final contribution that any early blastomere makes to the fate map in the gastrula cannot be predicted because of variability in both the position of the future dorsoventral axis with respect to the early cleavage blastomeres and the scattering of daughter cells as the gastrula is formed. Therefore, early cell divisions of the zebrafish embryo cannot reproducibly segregate determinants of tissue fates.

Defining how and when cell fate is determined is essential to understanding the mechanisms underlying development. In the zebrafish embryo, cell lineage analysis has shown that it is not until the early gastrula stage that cellular fate appears restricted, in that individual cells give rise to only single tissue types (1). The type of tissue formed by the descendants of an early gastrula cell can be generally predicted by the position of the cell within the early gastrula embryo, yielding a fate map for the zebrafish (2) (Fig. 1A). Because a tissue-specific fate map cannot be derived before this stage and there is little cell movement during the cleavage period, it has been proposed that extensive cell mixing occurs during the transition from blastula to gastrula (3, 4), such that a cell's position in the blastula is unrelated to the position of its descendants in the gastrula. In this model, the early blastomeres of the zebrafish are deemed to be pluripotent. Recent cell lineage results have challenged the

idea that extensive mixing occurs, suggesting that the position of an early blastomere is a reliable predictor of some aspects of later cell fate (5). A further conclusion from the latter work was that the body axes of the embryo can be predicted as early as the eight-cell stage. Here we resolve the issue of how the position of a cleavage blastomere relates to the distribution of its clonal descendants in the gastrula. We demonstrate that descendants of early blastomeres do not have predictable positions relative to the dorsoventral axis of the embryo. Thus, their prospective fates are not identifiable. In addition, we demonstrate that portions of the embryo retain their relative positions from blastula to gastrula, allowing some aspects of the zebrafish fate map to be observable at times earlier than the gastrula stage.

In the gastrula, a cell's position relative to the dorsal midline and along the animal-vegetal axis allows the fate of that cell to be predicted (Fig. 1A). For example, cells at the dorsal margin of the early gastrula have a specialized role in organizing the primary axis of the embryo (6). We have directly tested whether the position of early blastomeres correlates with the dorsoventral

Department of Human Genetics, Eccles Institute of Human Genetics, University of Utah, Salt Lake City, UT 84112, USA.

*These colleagues contributed equally to this work. †To whom correspondence should be addressed.

position of their descendants in the gastrula by examining the position of the dorsoventral axis relative to the second cleavage plane. Because the location of the dorsal side of the embryo cannot be determined biochemically or morphologically until the early gastrula stage, we developed a way to recognize the position of the second cleavage plane in gastrula-stage embryos. The position of the second cleavage plane is unambiguous at early times because of the regular pattern of the first few cleavages (7), but it becomes increasingly difficult to recognize once cells begin moving during epiboly and gastrulation. We identified (8) the position of the second cleavage plane in gastrula-stage embryos by labeling with lineage tracer dyes two end blastomeres at the eight-cell stage. The second cleavage plane separates these two cells and lies between the two labeled clones in the gastrula (yellow line in Fig. 1B). We used the dorsal-specific expression of *gooseoid* (9) to establish the position of the incipient dorsoventral axis (black line in Fig. 1B). We measured (10) the smaller of the two angles between the position of the second cleavage plane and the dorsoventral axis (θ ; Fig. 1B). An early gastrula embryo in

which θ is 53° is shown (Fig. 1C).

If there is any fixed relation between the dorsoventral axis and the initial cleavage planes, then there would be a clustering of θ at a particular angle. Conversely, if no relation between them exists, θ would be different for each embryo. We observed a broad distribution of angles over the full range from 0° to 90° (mean of 43.7°) (Fig. 2). The median of the data is 46° , indicating that it is as likely that the dorsoventral axis will fall near the first cleavage plane as it is to fall perpendicularly, near the second cleavage plane. These data indicate that the initial cleavage planes are not regularly aligned with the future dorsoventral axis. Similar conclusions have been reached recently by others (11).

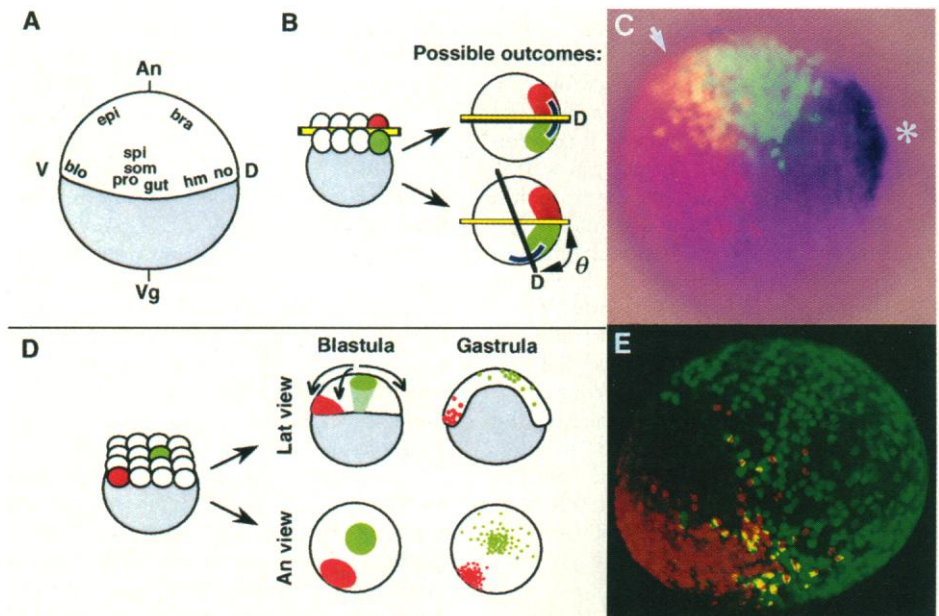
Our results are inconsistent with the possibility that the initial cleavages define the dorsoventral axis by strictly segregating cytoplasmic determinants. We note that these results do not indicate the time at which the dorsoventral axis is established. For example, the dorsoventral axis may be established early, in oocytes or cleaving embryos, and simply not correlate with the initial cleavage planes.

Others have reported either no correla-

tion (3), a slight bias (12, 13), or a strong bias (5) toward the second cleavage plane aligning with the dorsoventral axis. We offer two possible explanations for why our conclusions differ from those of other reports. First, our experiments allowed the simultaneous measurement of both the second cleavage plane and the dorsal midline. Second, the conclusions from some previous studies were based on an observed tendency for some blastomeres to populate only certain tissues, thus appearing restricted in their developmental potential. For example, it was found that a blastomere gave rise to left or right muscle, but that it rarely populated both sides simultaneously. Our experiments below were designed to explain this phenomenon. We demonstrate here that the tendency for blastomeres to populate discrete tissues is a result of limits on cell mixing and not necessarily due to axis specification.

We previously proposed (14) that during epiboly, the central core of the blastula mixes extensively but the margin of the blastula remains relatively unmixed (Fig. 1D). We predicted that as a consequence of this mixing pattern each early blastomere does not contribute equally to all regions of

Fig. 1. Fate map and analyses of how blastomeres contribute to the fate map. (A) A fate map for the zebrafish gastrula embryo (2). The top hemisphere indicates the blastoderm; the shaded lower hemisphere is the uncleaved yolk cell. Ectodermal fates arise from the animal pole region; mesodermal and endodermal fates arise from the margin of the blastoderm. Abbreviations: An, animal pole; Vg, vegetal pole; D, dorsal; V, ventral; bra, brain; blo, blood; epi, epidermis; hm, head muscle; no, notochord; pro, pronephros; som, somitic muscle; spi, spinal cord. (B) Experimental design to determine the relation between the second cleavage plane and the dorsoventral axis. At the eight-cell stage two end cells separated by the second cleavage plane were injected with red or green fluorescent lineage tracer dyes. The embryos were allowed to develop to the gastrula stage and were analyzed in animal pole views to detect cells of each clone as well as cells that expressed *gooseoid*. The yellow line indicates the second cleavage plane, the blue arc indicates *gooseoid* expression, and the black line indicates the dorsoventral axis. The smaller of the two angles (θ) between the two planes was measured ($n = 40$) such that θ can have any value from 0° to 90° . Two types of possible outcomes are illustrated: $\theta = 0^\circ$ (coincidence between the second cleavage plane and the dorsoventral axis) and $\theta = 68^\circ$. (C) An animal pole view of an embryo prepared as in (B) to analyze the relative positions of the dorsoventral axis and the second cleavage plane. The expression of *gooseoid* is a black arc, the asterisk indicates the approximate position of the dorsal midline, and the arrow indicates the approximate position of the second cleavage plane (identified by the region of overlap (yellow) between the red and green clones); $\theta = 53^\circ$. (D) Experimental design to measure the amount of scattering of cells in the central and marginal regions of the blastula as a consequence of epiboly. In this experiment, one central (green) and one corner marginal (red) cell were injected in each 16-cell embryo. The blastula is formed



during development by synchronous cell divisions that occur without cell movements, so that cells that are related by lineage form coherent clones within the embryo (3). At the onset of epiboly, the yolk bulges up into the blastoderm, the central region of the blastoderm thins and spreads, and the blastoderm margin migrates vegetally, yielding an inverted cup-shaped embryo (4). Lateral (Lat) views highlight the shape change of the embryo. The lateral cross section of the gastrula illustrates how marginal cells may stay more clustered than central cells. Animal pole (An) views highlight how two clones of the same size in the blastula scatter to different degrees in the gastrula. (E) A typical example of central and marginal clone scatter. Animal pole view of a mid-gastrula-stage embryo injected as described in (D). The dispersal of central (green) cells is more extensive than the dispersal of marginal (red) cells.

the fate map. To demonstrate whether epiboly and gastrulation are characterized by regional differences in cell mixing, we examined at the gastrula stage the clonal descendants of cells marked at the 16-cell stage (Fig. 1D). The 16-cell stage is the first time that cells giving rise to the central core of the blastula (the four inner cells) are fully separate from cells that contribute to the margin of the blastula (the 12 outer cells).

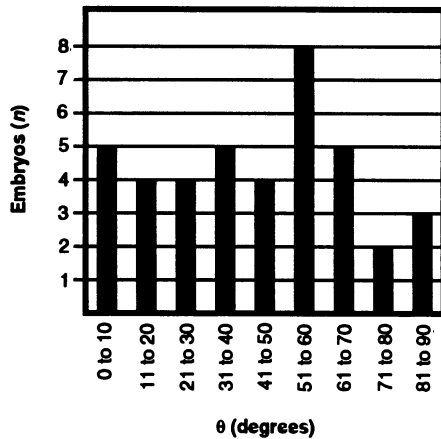


Fig. 2. The distribution of θ , the angle between the second cleavage plane and the dorsoventral axis, in 40 embryos. The mean was 43.7° (early gastrula = 44.6° , $n = 9$; mid-gastrula = 43.4° , $n = 31$), and the median was 46° .

Each embryo was injected with two different fluorescent dyes, one into a marginal cell and the other into a central cell (Fig. 1D). In a typical example (Fig. 1E), the inner clone (green) has scattered considerably more than the marginal clone (red). The two clones occupy distinct regions in the gastrula. Because position in the gastrula correlates with future tissue fate, we conclude that the fates of 16-cell blastomeres are not equivalent. In general, descendants of central cells spread extensively, covering the animal pole region and sometimes scattering to the margin (Figs. 1E and 3F). Relatively discrete borders were observed between labeled and unlabeled regions; that is, the descendants of each central cell do not mix thoroughly enough to be spread evenly over the entire gastrula.

A prominent subset of the descendants of injected marginal blastomeres did not scatter extensively (Figs. 1E and 3, A to E); each clone included a densely labeled region at the margin of the gastrula. As the clones populate limited regions of the margin of the gastrula, we conclude that each marginal cleavage blastomere gives rise to only a subset of the marginally derived embryonic tissues (see Fig. 1A). Scatter of clonal descendants away from the margin ranged continuously from minimal to extensive. The four types of scatter morphology illustrated (Fig. 3, A to D) were

observed in approximately equal numbers. Occasionally a marginal clone took on an extended, almost linear shape (Fig. 3E). We suggest that this morphology resulted from the effects of the gastrulation movements of involution and convergent extension (4, 15) on a marginal clone located at the dorsal midline.

Whether a marginal blastomere's descendants scatter a little or a lot, the embryo develops normally. This result is consistent with the notion that blastomeres are pluripotent and their fates reflect the eventual positions their descendants occupy in the early gastrula. Cell transplantation experiments (16) have illustrated that early gastrula cells do retain pluripotency and that they can regulate their fates in response to positional cues in the gastrula.

The difference in central and marginal clone scatter was quantified by examination of the relative projected area occupied by the two types of clones. We calculated (17) that the marginal clones occupy an area only $68.1 \pm 13.6\%$ as large as the area occupied by the central cell clones. This number underestimates the difference in area between the two types of clones, because we were unable to measure the entire extent of a scattered central clone in one field of view (17). Because the comparison of clone dispersal was always made between two clones in the same embryo, any potential differences in the ages of the two clones or in the overall size of each embryo were eliminated. By counting dissociated blastomeres from embryos injected as in Fig. 1D, we have established that the number of cells in the two types of clones are approximately equal and that each labeled clone represents approximately one-sixteenth of the total number of cells (18), as expected if each 16-cell blastomere expands similarly through the mid-gastrula stage (19).

We conclude that the marginal and animal pole regions of the gastrula are generated from largely different subsets of the early blastomeres. Any portion of the margin of the gastrula is populated by the descendants of only a few marginal blastomeres, with a minor contribution by the descendants of central blastomeres. The animal pole region of the gastrula is formed primarily by a mixture of the descendants of the four central blastomeres. Because marginal clones scatter to different degrees (Fig. 3), a variable number of marginal cell descendants contribute to the animal pole region of the embryo. Therefore, central and marginal blastomeres, by virtue of their positions in the cleavage stage, give rise to significantly different sets of embryonic fates.

By demonstrating that different types of cell mixing occur in central versus marginal regions, our work resolves why previous experiments generated conflicting conclusions. Kimmel and colleagues (3, 12) observed extensive cell scattering among descendants of nonmarginal cleavage blas-

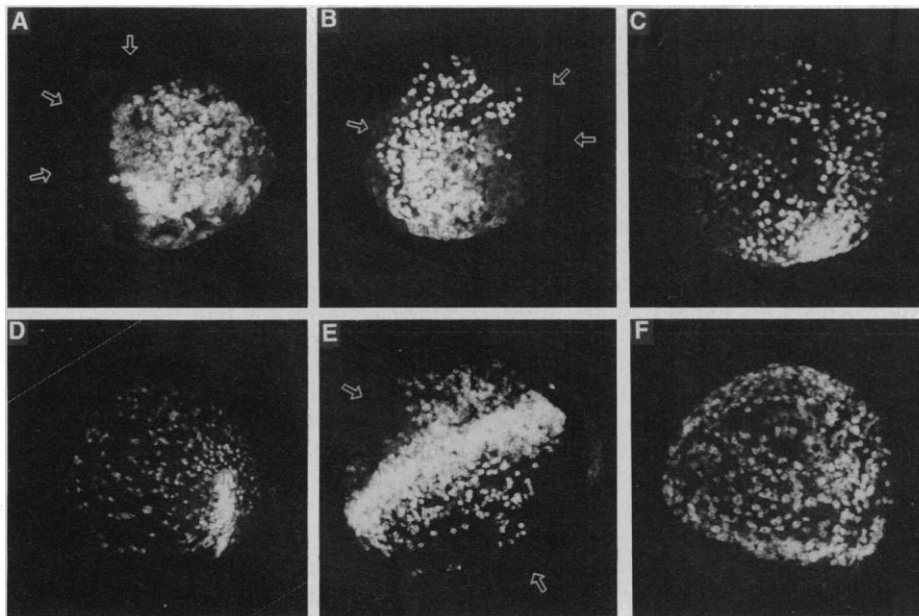


Fig. 3. The morphologies of marginal and central clone scatter. Sixteen-cell embryos ($n = 24$) were injected as in Fig. 1D and allowed to develop to the mid-gastrula stage. Images represent the projected Z-series of lateral views of single clones in each embryo. Embryos were oriented to show maximum scatter. Where few or no labeled cells extend to the edge of the blastoderm, arrows indicate the edge of the embryo. Equal numbers of injected embryos were observed whose marginal descendants scattered (A) very little, (B) a small amount, (C) a moderate amount, or (D) a large amount (though still with a densely populated portion of the clone at the margin). (E) Infrequently, a marginal clone displayed an extended, linear morphology. (F) Scatter of a typical central clone. In general, central clones were distributed uniformly, though rare central clones occasionally showed a region more densely populated than the rest of the clone.

tomeres, consistent with our finding that it is the central, nonmarginal region of the blastula that undergoes extensive cell mixing during epiboly. Strehlow and Gilbert (5) observed that the descendants of each eight-cell blastomere gave rise to a limited array of mesodermal tissues. These tissues arise at the margin, where we have observed limited cell mixing.

In sum, the descendants of each cleavage blastomere reside in a limited region of the gastrula and, therefore, populate only a subset of the possible cell fates. The particular subset of fates expressed depends on the position of the original blastomere relative to the future dorsoventral axis of the embryo. Because the dorsoventral axis is not fixed with respect to the early cleavage planes and the scatter of clones varies from embryo to embryo, the specific fate of any blastomere cannot be predicted at the cleavage stage.

REFERENCES AND NOTES

- C. B. Kimmel and R. M. Warga, *Science* **231**, 365 (1986).
- _____ and T. F. Schilling, *Development* **108**, 581 (1990).
- C. B. Kimmel and R. D. Law, *Dev. Biol.* **108**, 94 (1985).
- R. M. Warga and C. B. Kimmel, *Development* **108**, 569 (1990).
- D. Strehlow and W. Gilbert, *Nature* **361**, 451 (1993).
- H. Spemann and H. Mangold, *Wilhelm Roux Arch. Entwicklunsgsmech. Org.* **100**, 599 (1924); J. A. Oppenheimer, *J. Exp. Zool.* **72**, 409 (1936).
- C. B. Kimmel and R. D. Law, *Dev. Biol.* **108**, 78 (1985).
- Zebrafish (*Danio rerio*, Ekkwill Waterlife Resources, Gibsonton, FL) were maintained according to standard methods [M. Westerfield, Ed., *The Zebrafish Book* (Univ. of Oregon Press, Eugene, OR, 1993)]. Blastomeres were injected with fluorescein isothiocyanate-Dextran (2-megadalton molecular weight; Sigma) or Texas Red isothiocyanate-Dextran (2-megadalton molecular weight; Molecular Probes), prepared as described (5). Microinjection was performed under a stereomicroscope at a magnification of $\times 50$. Dechorionated embryos were placed in 60-mm petri plates coated with 1% agarose in Instant Ocean salts (150 mg/liter). A V-shaped trough cut in the agarose was used to hold the embryos for microinjection. Embryos were transferred to agarose-coated dishes and placed at 28.5°C to develop. Injected embryos were screened with a Zeiss Axioplan microscope with epifluorescence optics within 20 min after microinjection and again 3 to 4 hours later. Embryos were discarded if (i) fluorescence was found in the yolk or in incorrect blastomeres, (ii) blastomeres contained both dyes, (iii) parts of labeled clones fluoresced with variable intensity, or (iv) embryos had abnormal morphology. In each injection batch, up to 20% of injected embryos were discarded. Injected embryos raised to 48 hours developed normally. Embryos were fixed in freshly prepared 4% paraformaldehyde (Polysciences, Niles, IL) in sucrose fix buffer (M. Westerfield, above).
- S. E. Stachel, D. J. Grunwald, P. Z. Myers, *Development* **117**, 1261 (1993). Expression of *gooseoid* was detected by whole mount in situ hybridization as cited therein.
- Embryos were oriented with the animal pole upward in 3% methyl cellulose. Fluorescence optics were used to observe the labeled clones; bright-field optics were used to observe *gooseoid* staining. Photographs of the embryos were traced so that the positions of the two labeled clones could be analyzed in relation to the dorsal midline. The position of the second cleavage plane was defined as the midpoint between the overlap of the two clones. The borders of each clone and the region of overlap could be viewed most clearly with fluorescence optics in the absence of white light. On average, the region of overlap covered an arc of 35°. The position of the dorsoventral axis was determined by drawing a line through the center of the gastrula and the midpoint of either the arc of *gooseoid* staining in early gastrula (40% epiboly) embryos or the center of the dot of *gooseoid* staining in midgastrula (60% epiboly) embryos. As expected, in half the embryos the region of overlap between the labeled clones fell on the ventral side of the embryo.
- S. Abdellilah, L. Solnica-Krezel, D. Stainier, W. Driever, *Nature*, in press.
- C. B. Kimmel and R. M. Warga, *Dev. Biol.* **124**, 269 (1987).
- J. A. Oppenheimer, *J. Exp. Zool.* **73**, 405 (1936).
- E. T. Wilson, K. A. Helde, D. J. Grunwald, *Trends Genet.* **9**, 348 (1993).
- C. B. Kimmel, R. M. Warga, D. A. Kane, *Development* **120**, 265 (1994).
- R. K. Ho and C. B. Kimmel, *Science* **261**, 109 (1993); S. Schulte-Merker, R. K. Ho, B. G. Herrmann, C. Nusslein-Volhard, *Development* **116**, 1021 (1992).
- Embryos were injected as in Fig. 1D, allowed to develop to 60 to 75% epiboly, then fixed and mounted as described above. Observations were by Bio-Rad confocal laser scanning microscopy (MRC-600); projected Z-series were analyzed. Each embryo was oriented twice to show the central and marginal clones separately. The area occupied by each labeled clone was defined as the portion of the clone with pixel intensities within the range of 43 to 255, from the Histogram function of the software CoMOS 6.01 (Bio-Rad). For each embryo, the ratio (area of marginal clone/area of central clone) between the two areas was calculated. The mean of the ratios ($n = 22$) was determined after the most extreme high and low values were discarded. The spread of central clones was so extensive that only a portion could be captured in a single Z-series. In contrast, the vast majority of each marginal clone could be examined in a single orientation. As such, the ratio of the areas is an underestimate of the difference in scatter between the two types of clones.
- Embryos were injected as described in Fig. 1D. At 60% epiboly, eight embryos were dissociated into single cells in Ca^{2+} -, Mg^{2+} -free phosphate buffered saline and fixed as described above. The dissociated cells of each embryo were treated with 4,6-diamine-2-phenylindole (DAPI) to label all nuclei. For each embryo, about 300 DAPI-positive cells were analyzed to identify cells also labeled with fluorescein or Texas Red.
- Early cell division in the zebrafish is rapid and synchronous (7); later divisions are slower, asynchronous, and do not cluster in a particular region of the embryo [D. A. Kane and C. B. Kimmel, *Development* **119**, 447 (1993); D. A. Kane, R. M. Warga, C. B. Kimmel, *Nature* **360**, 735 (1992)].
- We thank the members of our lab and the Department of Human Genetics for stimulating discussions during the course of these experiments as well as C. Thummel and P. Reid for their generosity and technical support. K.A.H. is a predoctoral trainee supported by a National Institutes of Health training grant. D.J.G. was supported by a Sloan Fellowship. Supported by grants from the University of Utah and the National Science Foundation (DCB-9105585).

13 May 1994; accepted 24 June 1994

The High-Resolution Crystal Structure of a Parallel-Stranded Guanine Tetraplex

Gerard Laughlan, Alastair I. H. Murchie, David G. Norman, Madeleine H. Moore, Peter C. E. Moody, David M. J. Lilley, Ben Luisi

Repeat tracts of guanine bases found in DNA and RNA can form tetraplex structures in the presence of a variety of monovalent cations. Evidence suggests that guanine tetraplexes assume important functions within chromosomal telomeres, immunoglobulin switch regions, and the human immunodeficiency virus genome. The structure of a parallel-stranded tetraplex formed by the hexanucleotide d(TG₄T) and stabilized by sodium cations was determined by x-ray crystallography to 1.2 angstroms resolution. Sharply resolved sodium cations were found between and within planes of hydrogen-bonded guanine quartets, and an ordered groove hydration was observed. Distinct intra- and intermolecular stacking arrangements were adopted by the guanine quartets. Thymine bases were exclusively involved in making extensive lattice contacts.

DNA and RNA containing runs of consecutive guanine bases may adopt four-stranded conformations based on the hydrogen-bonded

guanine tetrad, or G quartet (1–4). These conformations may exist in a variety of isomeric forms, encompassing both parallel and antiparallel conformations, all of which are stabilized by monovalent ions such as sodium and potassium (2, 5, 6). Such tetraplexes have been implicated in a variety of biological roles, including the function of chromosome telomeres (7), the dimerization of the human immunodeficiency virus RNA genome (8), and the site-specific recombination of immunoglobulin genes (1), and their functional

G. Laughlan and B. Luisi, Medical Research Council Virology Unit, Church Street, University of Glasgow, Glasgow G11 5JR, UK.

A. I. H. Murchie, D. G. Norman, D. M. J. Lilley, Cancer Research Campaign, Nucleic Acid Structure Research Group, Department of Biochemistry, The University, Dundee DD1 4HN, UK.

M. H. Moore and P. C. E. Moody, Department of Chemistry, York University, Heslington, York YO1 5DD, UK.